
AMBER: Adaptive Multi-Batch Experience Replay for Continuous Action Control

Seungyul Han

Dept. of Electrical Engineering
KAIST
Daejeon, South Korea 34141
sy.han@kaist.ac.kr

Youngchul Sung[†]

Dept. of Electrical Engineering
KAIST
Daejeon, South Korea 34141
ycsung@kaist.ac.kr

Abstract

In this paper, a new adaptive multi-batch experience replay scheme is proposed for proximal policy optimization (PPO) for continuous action control. On the contrary to original PPO, the proposed scheme uses the batch samples of past policies as well as the current policy for the update for the next policy, where the number of the used past batches is adaptively determined based on the oldness of the past batches measured by the average importance sampling (IS) weight. The new algorithm constructed by combining PPO with the proposed multi-batch experience replay scheme maintains the advantages of original PPO such as random mini-batch sampling and small bias due to low IS weights by storing the pre-computed advantages and values and adaptively determining the mini-batch size. Numerical results show that the proposed method significantly increases the speed and stability of convergence on various continuous control tasks compared to original PPO.

1 Introduction

Reinforcement learning (RL) aims to optimize the policy for the cumulative reward in a Markov decision process (MDP) environment. SARSA and Q-learning are well-known RL algorithms for learning finite MDP environments, which store all Q values as a table and solve the Bellman equation [12, 17, 21]. However, if the state space of environment is infinite, all Q values cannot be stored. Deep Q-learning (DQN) [10] solves this problem by using a Q-value neural network to approximate and generalize Q-values from finite experiences, and DQN is shown to outperform the human level in Atari games with discrete action spaces [11]. For discrete action spaces, the policy simply can choose the optimal action that has the maximum Q-value, but this is not possible for continuous action spaces. Thus, policy gradient (PG) methods that parameterize the policy by using a neural network and optimize the parameterized policy to choose optimal action from the given Q-value are considered for continuous action control [18]. Recent PG methods can be classified mainly into two groups: 1) Value-based PG methods that update the policy to choose action by following the maximum distribution or the exponential distribution of Q-value, e.g., deep deterministic policy gradient (DDPG) [7], twin-delayed DDPG (TD3) [5], and soft-actor critic (SAC) [6], and 2) IS-based PG methods that directly update the policy to maximize the discounted reward sum by using IS, e.g., trust region policy optimization (TRPO) [14], actor-critic with experience replay (ACER) [20], PPO [16]. Both PG methods update the policy parameter by using stochastic gradient descent (SGD), but the convergence speed of SGD is slow since the gradient direction of SGD is unstable. Hence, increasing sample efficiency is important to PG methods for fast convergence. Experience replay (ER), which was first considered in DQN [10], increases sample efficiency by storing old sample from the previous policies and reusing these old samples for current update, and enhances the learning stability by reducing the sample correlation by sampling random mini-batches from a large replay memory. For value-based PG methods, ER can be applied without any modification, so state-of-the-art value-based

algorithms (TD3, SAC) use ER. However, applying ER to IS-based PG methods is a challenging problem. For IS-based PG methods, calibration of the statistics between the sample-generating old policies and the policy to update is required through IS weight multiplication [3], but using old samples makes large IS weights and this causes large variances in the empirical computation of the loss function. Hence, TRPO and PPO do not consider ER, and ACER uses clipped IS weights with an episodic replay to avoid large variances, and corrects the bias generated from the clipping [20].

In this paper, we consider the performance improvement for IS-based PG methods by reusing old samples appropriately based on IS weight analysis and propose a new adaptive multi-batch experience replay (MBER) scheme for PPO, which is currently one of the most popular IS-based PG algorithms. PPO applies clipping but ignores bias, since it uses the sample batch (or horizon) only from the current policy without replay and hence the required IS weight is not so high. On the contrary to PPO, the proposed scheme uses the batch samples of past policies as well as the current policy for the update for the next policy, and applies proper techniques to preserve most advantages of PPO such as random mini-batch sampling and small bias due to low IS weights. The details of the proposed algorithm will be explained in coming sections.

Notations: $X \sim P$ means that a random variable X follows a probability distribution P . $\mathcal{N}(\mu, \sigma^2)$ denotes the Gaussian distribution with mean μ and variance σ^2 . $\mathbb{E}[\cdot]$ denotes the expectation operator. τ_t denotes a state-action trajectory from time step t : $(s_t, a_t, s_{t+1}, a_{t+1}, \dots)$.

2 Background

2.1 Reinforcement Learning Problems

In this paper, we assume that the environment is an MDP. $\langle \mathcal{S}, \mathcal{A}, \gamma, P, r \rangle$ defines a discounted MDP, where \mathcal{S} is the state space, \mathcal{A} is the action space, γ is the discount factor, P is the state transition probability, and r is the reward function. For every time step t , the agent chooses an action a_t based on the current state s_t and then the environment gives the next state s_{t+1} according to P and the reward $r_t = r(s_t, a_t)$ to the agent. Reinforcement learning aims to learn the agent's policy $\pi(a_t|s_t)$ that maximizes the average discounted return $J = \mathbb{E}_{\tau_0 \sim \pi}[\sum_{t=0}^{\infty} \gamma^t r_t]$.

2.2 Deep Q-Learning and PG Methods

Q-learning is a widely-used reinforcement learning algorithm based on the state-action value function (Q-function). The state-action value function represents the expected return of a state-action pair (s_t, a_t) when a policy π is used, and is denoted by $Q_\pi(s_t, a_t) = \mathbb{E}_{\tau_t \sim \pi}[\sum_{l=t}^{\infty} \gamma^l r_l]$ [17]. To learn the environment with a discrete action space, DQN approximates the Q-function by using a Q-network $Q_w(s_t, a_t)$ parameterized by w , and defines the deterministic policy $\pi(a|s) = \arg \max_{a \in \mathcal{A}} Q_w(s, a)$. Then, DQN updates the Q-network parameter w to minimize the temporal difference (TD) error:

$$(r_t + \gamma \max_{a'} Q_{w'}(s_{t+1}, a') - Q_w(s_t, a_t))^2, \quad (1)$$

where w' is the target network. (1) is from the result of the value iteration algorithm which finds an optimal policy by using the Bellman equation [10]. Note that the TD error requires maximum of Q-function, but it cannot be computed in a continuous action space. To learn a continuous action environment, PG directly parameterizes the policy by a stochastic policy network $\pi_\theta(a_t|s_t)$ with parameter θ and sets an objective function $L(\theta)$ to optimize the policy: Value-based PG methods set $L(\theta)$ as the policy follows some distribution of Q-function [5–7], and IS-based PG methods set $L(\theta)$ as the discounted return and directly updates the policy to maximize $L(\theta)$ [14, 16].

2.3 IS-based PG and PPO

At each iteration, IS-based PG such as ACER and simple PPO¹ tries to obtain a better policy $\pi_{\tilde{\theta}}$ from the current policy π_{θ} [14]:

$$\begin{aligned} L_{\theta}(\tilde{\theta}) &\triangleq \mathbb{E}_{s_t \sim \rho_{\pi_{\theta}}, a_t \sim \pi_{\tilde{\theta}}} [A_{\pi_{\theta}}(s_t, a_t)] \\ &= \mathbb{E}_{s_t \sim \rho_{\pi_{\theta}}, a_t \sim \pi_{\theta}} \left[R_t(\tilde{\theta}) A_{\pi_{\theta}}(s_t, a_t) \right], \end{aligned} \quad (2)$$

where $A_{\pi_{\theta}}(s_t, a_t) = Q_{\pi_{\theta}}(s_t, a_t) - V_{\pi_{\theta}}(s_t)$ is the advantage function, $V_{\pi_{\theta}}(s_t) = \mathbb{E}_{a_t, \tau_{t+1} \sim \pi} [\sum_{l=t}^{\infty} \gamma^l r_l]$ is the state-value function, and $R_t(\tilde{\theta}) = \frac{\pi_{\tilde{\theta}}(a_t|s_t)}{\pi_{\theta}(a_t|s_t)}$ is the IS weight. Here, the objective function $L_{\theta}(\tilde{\theta})$ is a function of $\tilde{\theta}$ for given θ , and $\tilde{\theta}$ is the optimization variable. To compute $L_{\theta}(\tilde{\theta})$ empirically from the samples from the current policy π_{θ} , the IS weight is multiplied. That is, with $R_t(\tilde{\theta})$ multiplied to $A_{\pi_{\theta}}(s_t, a_t)$, the second expectation in (2) is over the trajectory generated by the current policy π_{θ} not by the updated policy $\pi_{\tilde{\theta}}$. Here, large IS weights cause large variances in (2), so ACER and PPO bound or clip the IS weight [16, 20]. In this paper, we use the clipped important sampling structure of PPO as our baseline. The objective function with clipped IS weights becomes

$$L_{CLIP}(\tilde{\theta}) = \mathbb{E}_{s_t \sim \rho_{\pi_{\theta}}, a_t \sim \pi_{\theta}} \left[\min\{R_t(\tilde{\theta})\hat{A}_t, \text{clip}_{\epsilon}(R_t(\tilde{\theta}))\hat{A}_t\} \right], \quad (3)$$

where $\text{clip}_{\epsilon}(\cdot) = \max(\min(\cdot, 1 + \epsilon), 1 - \epsilon)$ with clipping factor ϵ , and \hat{A}_t is the sample advantage function estimated by the generalized advantage estimator (GAE) [15]:

$$\hat{A}_t = \sum_{l=0}^{N-n-1} (\gamma\lambda)^l \delta_{t+l}, \quad (4)$$

where N is the number of samples in one iteration (horizon), $\delta_t = r_t + \gamma V_w(s_{t+1}) - V_w(s_t)$ with the state-value network $V_w(s_t)$ which approximates $V_{\pi_{\theta}}(s_t)$. Then, PPO updates the state-value network to minimize the square loss:

$$L_V(w) = (V_w(s_t) - \hat{V}_t)^2, \quad (5)$$

where \hat{V}_t is the TD(λ) return [16].

In [16], for continuous action control, a Gaussian policy network is considered, i.e.,

$$a_t \sim \pi_{\theta}(\cdot|s_t) = \mathcal{N}(\mu(s_t; \phi), \sigma^2), \quad (6)$$

where $\mu(s_t; \phi)$ is the mean neural network whose input is s_t and parameter is ϕ ; σ is a standard deviation parameter; and thus $\theta = (\phi, \sigma)$ is the overall policy parameter.

3 Related Works

3.1 Experience Replay on Q-Learning

Q-learning is off-policy learning which only requires sampled tuples to compute the TD error (1) [17]. DQN uses the ER technique [8] that stores old sample tuples (s_t, a_t, r_t, s_{t+1}) in replay memory \mathbf{R} and updates the Q-network with the average gradient of the TD error computed from a mini-batch uniformly sampled from \mathbf{R} . Value-based PG methods adopt this basic ER of DQN. As an extension of this basic ER, [13] considered prioritized ER to give a sampling distribution on the replay instead of uniform random sampling so that samples with higher TD errors are used more frequently to obtain the optimal Q faster than DQN. [9] analyzed the effect of the replay memory size on DQN and proposed an adaptive replay memory scheme based on the TD error to find a proper replay size for each discrete task. It is shown that this adaptive replay size for DQN enhances the overall performance.

¹We only consider simple PPO without adaptive KL penalty since simple PPO has the best performance on continuous action control tasks.

3.2 Experience Replay on IS-based PG

ER can be applied to IS-based PG for continuous action control to increase sample efficiency. As seen in (2), the multiplication of the IS weight $R_t(\tilde{\theta}) = \frac{\pi_{\tilde{\theta}}(a_t|s_t)}{\pi_{\theta}(a_t|s_t)}$ is required to use the samples from old policies for current policy update. In case that ER uses samples from many previous policies, the required IS weight is very large and this induces bias even though clipping is applied. The induced bias makes the learning process unstable and disturbs the computation of the expected loss function. Thus, ACER uses ER with bias correction, and proposes an episodic ER scheme that samples and stores on the basis of episodes because it computes an off-policy correction Q-function estimator which requires whole samples in a trajectory as Algorithm 3 in [20].

4 Multi-Batch Experience Replay

4.1 Batch Structures of ACER and PPO

Before introducing our new replay scheme, we compare the batch description of ACER and PPO for updating the policy, as shown in Fig. 1. ACER uses an episodic ER to increase sample efficiency. In the continuous action case, ACER stores trajectories from $V = 100$ previous policies and each policy generates a trajectory of $M = 50$ time steps in replay memory \mathbf{R} . For each update period, ACER chooses $W \sim \text{Poisson}(4)$ random episodes from \mathbf{R} to update the policy. Then, different statistics among the samples in the replay causes bias, and the episodic sample mini-batch is highly correlated. On the other hand, PPO does not use ER but collects a single batch of size $N = 2048$ time steps from the current policy. Then, PPO draws a mini-batch of size $M = 64$ randomly and uniformly from the single batch; updates the policy to the direction of the gradient of the empirical loss computed from the drawn mini-batch:

$$\hat{L}_{CLIP}(\tilde{\theta}) = \frac{1}{M} \sum_{m=0}^{M-1} \min\{R_m(\tilde{\theta})\hat{A}_m, \text{clip}_{\epsilon}(R_m(\tilde{\theta}))\hat{A}_m\}; \quad (7)$$

and updates the value network to the direction of the negative gradient of

$$\hat{L}_V(w) = \frac{1}{M} \sum_{m=0}^{M-1} (V_w(s_m) - \hat{V}_m)^2, \quad (8)$$

where \hat{A}_m , $R_m(\tilde{\theta})$, $V_w(s_m)$, and \hat{V}_m are values corresponding to the m -th sample in the mini-batch [16]. This procedure is repeated for 10 epochs for a single batch of size N .² Note that PPO uses current samples only, so it can ignore bias because the corresponding IS weights do not exceed the clipping factor mostly. Furthermore, the samples in a mini-batch drawn uniformly from the total batch of size N in PPO have little sample correlation because they are scattered over the total batch. However, PPO discards all samples from all the past policies except the current policy for the next policy update and this reduces sample efficiency.

4.2 The Proposed Multi-Batch Experience Replay Scheme

We now present our MBER scheme suitable to PPO-style IS-based PG, which increases sample efficiency, maintains random mini-batch sampling to diminish the sample correlation, and reduces the IS weight to avoid bias. We apply our MBER scheme to PPO to construct an enhanced algorithm named PPO-MBER, which includes PPO as a special case.

In order to obtain the next policy, the proposed scheme uses the batch samples of $L - 1$ past policies and the current policy, whereas original PPO uses the batch samples from only the current policy, as illustrated in Fig. 1. The stored information for MBER in the replay memory \mathbf{R} is as follows. To compute the required IS weight $R_t(\tilde{\theta}) = \frac{\pi_{\tilde{\theta}}(a_t|s_t)}{\pi_{\theta}(a_t|s_t)}$ for each sample in a random mini-batch, MBER stores the statistical information of every sample in \mathbf{R} . Under the assumption of a Gaussian policy network (6), the required statistical information for each sample is the mean $\mu_t := \mu(s_t; \phi)$ and the standard deviation σ . Furthermore, MBER stores the pre-calculated estimated advantage

²1 epoch means that we use every samples in the batch to update it once. In other words, PPO updates the policy by drawing $10 \cdot N/M$ mini-batches.

\hat{A}_t and target value \hat{V}_t of every sample in \mathbf{R} . Thus, MBER stores the overall sample information $(s_t, a_t, \hat{A}_t, \hat{V}_t, \mu_t, \sigma)$ regarding the batch samples from the most recent L policies, as described in Fig. 1. The storage of the statistical information (μ_t, σ) and the values (\hat{A}_t, \hat{V}_t) in addition to (s_t, a_t) for every sample in the replay memory makes it possible to draw a random mini-batch from \mathbf{R} not a trajectory like in ACER. Since the policy at the i -th iteration generates a batch of N samples, we can rewrite the stored information by using two indices $i = 0, 1, \dots$ and $n = 0, 1, \dots, N-1$ (such that time step $t = iN + n$) as $\{B_{i-L+1}, \dots, B_i\}$ from the most recent L policies $i, i-1, \dots, i-L+1$, where

$$B_i = (s_{i,n}, a_{i,n}, \hat{A}_{i,n}, \hat{V}_{i,n}, \mu_{i,n}, \sigma_i), \quad n = 0, \dots, N-1. \quad (9)$$

In addition to using the batch samples from most recent L policies, MBER enlarges the mini-batch size by L times compared to that of original PPO, to reduce the average IS weight. If we set the mini-batch size of MBER to be the same as that of PPO with the same epoch, then the number of updates of PPO-MBER is L times larger than that of PPO. Then, the updated policy statistic is too much different from the current policy statistic and thus the average IS weight becomes large as L increases. This causes bias and is detrimental to the performance. To avoid this, we enlarge the mini-batch size of MBER by L times and this reduces the average IS weight by making the number of updates the same as that of PPO with the same epoch. In this way, MBER can ignore bias without much concern, because its IS weight is similar to that of PPO. Fig. 2 shows the average IS weight³ of all sampled mini-batches at each iteration when $M = 64$ and $M = 64L$. It is seen that PPO-MBER maintains the same level of the important sampling weight as original PPO.

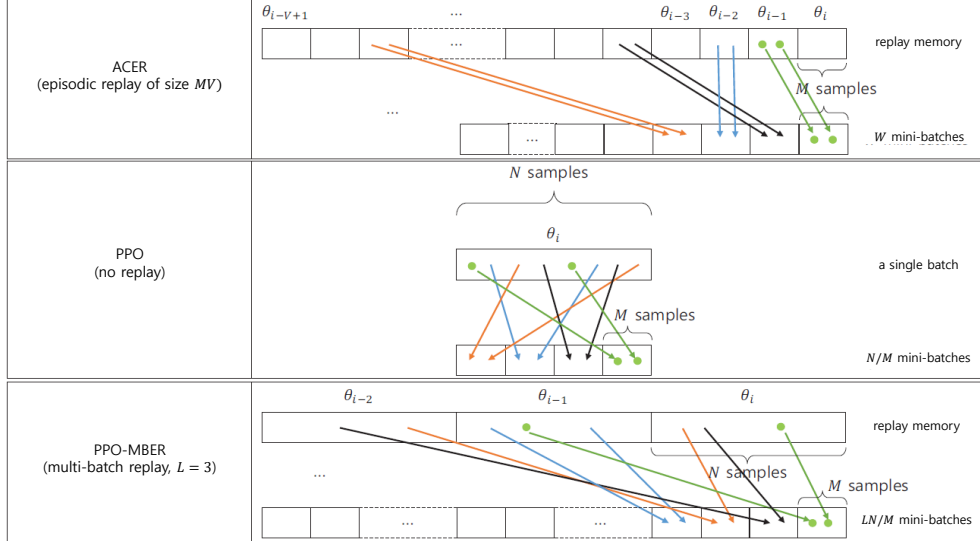


Figure 1: Batch construction of ACER, PPO and PPO with the proposed MBER (PPO-MBER): $N = 8$ and $M = 2$

5 Adaptive Batch Drop

PPO-MBER can significantly enhance the overall performance compared to PPO by using the MBER scheme, as seen in Section 7. However, we observe that the PPO-MBER performance for each task depends on the replay length L , and hence the choice of L is crucial to PPO-MBER. For the two extreme examples, Pendulum and Humanoid, in Table 3, note that the performance of Pendulum is proportional to the replay length but the performance of Humanoid is inversely proportional to the replay length. To analyze the cause of this phenomenon, we define the batch average IS weight between the old policy θ_{i-l} and the current policy θ_i as

$$R'_{i,l} = \frac{1}{N} \sum_{n=1}^{N-1} 1 + \text{abs} \left(1 - \frac{\pi_{\theta_i}(a_{i-l,n} | s_{i-l,n})}{\pi_{\theta_{i-l}}(a_{i-l,n} | s_{i-l,n})} \right), \quad (10)$$

³Actually, we averaged $\text{abs}(1 - R_m(\tilde{\theta})) + 1$ instead of $R_m(\tilde{\theta})$ to see the degree of deviation from 1.

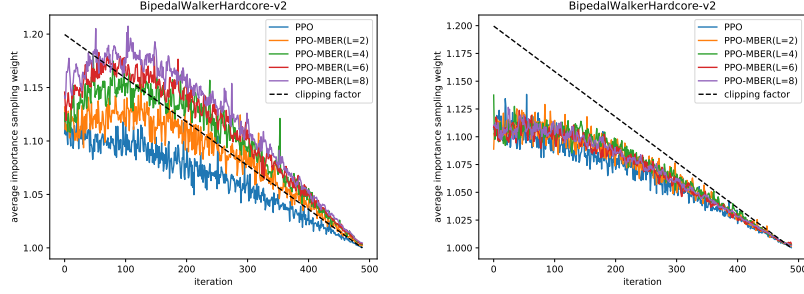


Figure 2: Average IS weight of BipedalWalkerHardcore for PPO-MBER: (Upper) $M = 64$, $\epsilon = 0.2$ and (Lower) $M = 64L$, $\epsilon = 0.2$

where $a_{i-l,n}$, $s_{i-l,n} \in B_{i-l}$. Note that this is different from the average of $1 + \text{abs}(1 - R_m(\tilde{\theta}))$ which depends on the updating policy $\pi_{\tilde{\theta}}$ not the current policy π_{θ_i} . Fig. 3 shows $R'_{i,l}$ of PPO-MBER for Pendulum, Humanoid, and BipedalWalkerHardcore tasks. It is seen that $R'_{i,l}$ increases as l increases, because the batch statistic is updated as iteration goes on. It is also seen that Humanoid has "large" $R'_{i,l}$ and Pendulum has "small" $R'_{i,l}$. From the two examples, it can be inferred that the batch samples B_{i-l} with large $R'_{i,l}$ are too old for updating $\tilde{\theta}$ at the current policy parameter θ_i and can harm the performance, as in the case of Humanoid. On the other hand, if $R'_{i,l}$ is small, more old samples can be used for update and this is beneficial to the performance. Therefore, it is observed in Table 3 that original PPO, i.e., $L = 1$ is best for Humanoid and PPO-MBER with $L = 8$ is best for Pendulum (In Table 3, we only consider L up to 8). Exploiting this fact, we propose an adaptive MBER (AMBER) scheme which adaptively chooses the batches to use for update from the replay memory. In the proposed AMBER, we store the batch samples from policies $\theta_i, \theta_{i-1}, \dots, \theta_{i-L+1}$, but use only the batches B_{i-l} 's whose $R'_{i,l}$ is smaller than the batch drop factor ϵ_b . Since $R'_{i,l}$ increases as time goes, AMBER uses the most recent L' sample batches whose $R'_{i,l}$ is less than ϵ_b . It is seen in Table 3 that PPO-AMBER well selects the proper replay length.

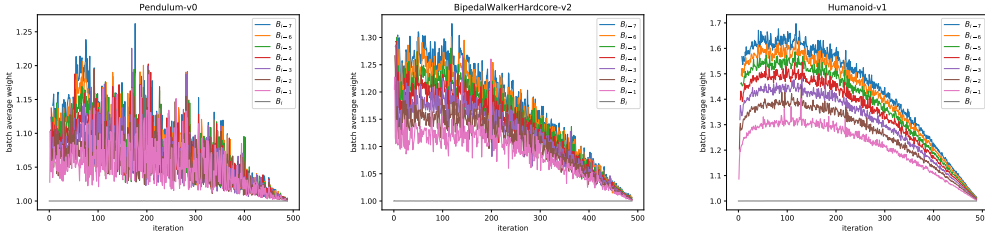


Figure 3: Batch average weight $R'_{i,l}$ of PPO-MBER ($L = 8$, $\epsilon = 0.4$): (Upper) Pendulum, (Center) BipedalWalkerHardcore, and (Lower) Humanoid

6 The Algorithm

Now, we present our proposed algorithm PPO-(A)MBER that maximizes the objective function $\hat{L}_{CLIP}(\tilde{\theta})$ in (7) for continuous action control. We assume the Gaussian policy network $\pi_{\tilde{\theta}}$ in (6) and the value network V_w . (They do not share parameters.) We define the overall parameter $\tilde{\theta}_{ALL}$ combining the policy parameter $\tilde{\theta}$ and the value parameter w . The objective function is given by [16]

$$\hat{L}(\tilde{\theta}_{ALL}) = \hat{L}_{CLIP}(\tilde{\theta}) - c_v \hat{L}_V(w), \quad (11)$$

where $\hat{L}_{CLIP}(\tilde{\theta})$ is in (7), $\hat{L}_V(w)$ is in (8), and c_v is a constant (we use $c_v = 1$ in the paper). The algorithm is summarized as Algorithm 1 in Appendix.

7 Experiments

7.1 Environment Description and Parameter Setup

To evaluate our ER scheme, we conducted numerical experiments on OpenAI GYM environments [1]. We selected continuous action control environments of GYM: Mujoco physics engines [19], classical control, and Box2D [2]. The dimensions of state and action for each task are described in Table 1. We used PPO baselines of OpenAI [4] and compared the performance of PPO-(A)MBER with

Table 1: Description of Continuous Action Control Tasks

Mujoco Tasks	State dim.	Action dim.
HalfCheetah-v1	17	6
Hopper-v1	11	3
HumanoidStandup-v1	376	17
Humanoid-v1	376	17
InvertedDoublePendulum-v1	11	1
InvertedPendulum-v1	4	1
Swimmer-v1	8	2
Reacher-v1	11	2
Walker2d-v1	17	6
Classic Control	State dim.	Action dim.
Pendulum-v0	3	1
Box2D	State dim.	Action dim.
BipedalWalker-v2	24	4
BipedalWalkerHardcore-v2	24	4

various replay lengths $L = 1$ (PPO), 2, 4, 6, 8 on continuous action control tasks in Table 1. The hyperparameters of PPO/PPO-MBER are described in Table 2: Adam step size β and clipping factor ϵ decay linearly as time-step goes on from the initial values to 0. The Gaussian mean network and the value network are feed-forward neural networks that have 2 hidden layers of size 64 like in [16]. For all the performance plots/tables in this paper, we performed 10 simulations per each task with random seeds. For each performance plot, the X -axis is time step, the Y -axis is the average return of the latest 100 episodes at each time step, and the line in the plot is the mean performance of 10 random seeds. For each performance table, results are described as the mean \pm one standard deviation of 10 seeds and the best scores are in boldface. To measure the overall performance of an algorithm on various continuous control tasks, we first compute the normalized score (NS) over all simulation setups in this paper for each task, then compute the average NS (ANS) which is the averaged over all tasks like in [16]. It can be thought that the ANS of final 100 episodes indicates the performance after convergence and the ANS of all episodes indicates the speed of convergence. We refer to the former as the final ANS and the latter as the speed ANS. The ANS results of all simulation settings in this paper are summarized in Appendix.

7.2 Performance and Ablation Study of PPO-MBER

In [16], the optimal clipping factor is 0.2 for PPO. However, it depends on the task set. Since our task set is a bit different from that in [16], we first evaluated the performance of PPO and PPO-MBER by sweeping the clipping factor from $\epsilon = 0.2$ to $\epsilon = 0.7$, and the corresponding final/speed ANS results are summarized in Tables 5 and 7, respectively. From the results, we observe that loosening the clipping factor a bit is beneficial for both PPO and PPO-MBER in the considered set of tasks, especially PPO-MBER with larger replay lengths. This is because loosening the clipping factor reduces the bias and increases the variance of the loss expectation, but a larger mini-batch of PPO-MBER reduces the variance by offsetting⁴. However, too large a clipping factor harms the performance. The best clipping factor is $\epsilon = 0.3$ for PPO and $\epsilon = 0.4$ for PPO-MBER. The detailed

⁴One may think that PPO with a large mini-batch size also has the same effect, but enlarging the mini-batch size without increasing the replay memory size increases the sample correlation and reduces the number of updates too much, so it is not helpful for PPO.

score for each task for PPO and PPO-MBER with the best clipping factors is given in Table. 3 and 4. The PPO results match with those in [16] for most environments, but note that the Swimmer performance of PPO in our result is a little worse than that of [16]. This is because PPO sometimes fails to perfectly learn the environment as the number of random seeds increases from 3 of [16] to 10 of ours. However, PPO-MBER learns the Swimmer environment more stably since it averages more samples based on enlarged mini-batches, so there is a large performance gap in this case. It is observed that in most environments, PPO-MBER with proper L significantly enhances both the final and speed ANS results as compared to PPO.

We then investigated the performance of random mini-batches versus episodic mini-batches for PPO-MBER with $L = 2$, $\epsilon = 0.4$. In the episodic case, we draw each mini-batch by picking a consequent trajectory of size M like ACER. Fig. 4 shows the results under several environments. It is seen that there is a notable performance gap between the two cases. This means that random mini-batch drawing from the replay memory storing pre-computed advantages and values in MBER has the advantage of reducing the sample correlation in a mini-batch and this is beneficial to the performance.

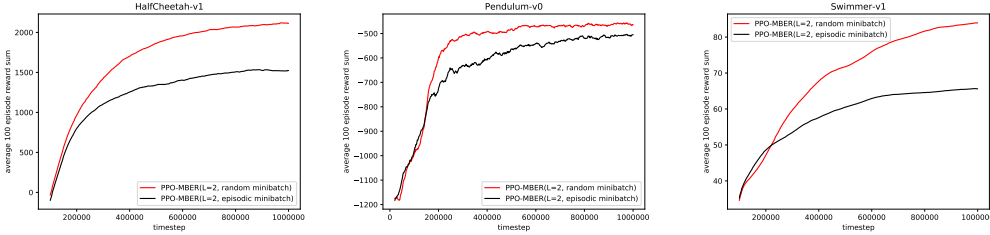


Figure 4: Performance comparison of HalfCheetah, Pendulum, and Swimmer for PPO-MBER ($L = 2$, $\epsilon = 0.4$) with uniformly random mini-batch and episodic mini-batch

7.3 Performance of PPO-AMBER

From the ablation study in the previous subsection, we set $\epsilon = 0.4$, which is good for a wide range of tasks, and set $L = 8$ as the maximum replay size for PPO-AMBER. PPO-AMBER shrinks the mini-batch size as $M = 64 \times \#$ of active batches, as shown in Algorithm 1, and other parameters are the same as those of PPO-MBER, as shown in Table 2. The batch drop factor ϵ_b is linearly annihilated from the initial value to zero as time step goes on. To search for optimal batch drop factor, we sweep the initial value of the batch drop factor from 0.1 to 0.3 and the corresponding ANS result of PPO-AMBER is provided in Table 6 and 8. In addition, Fig. 5 shows the number of active batches of PPO-AMBER for various batch drop factors for Pendulum, BipedalWalkerHardcore, and Humanoid tasks. It is seen from the result that $\epsilon_b = 0.25$ seems appropriate. Tables 3 and 4 and Fig. 6 show the performance of PPO ($\epsilon = 0.3$), PPO-MBER ($\epsilon = 0.4$), and PPO-AMBER ($L = 8$, $\epsilon = 0.4$, $\epsilon_b = 0.25$) on various tasks. It is seen that PPO-AMBER with $\epsilon_b = 0.25$ automatically selects almost optimal replay size from $L = 1$ to $L = 8$. So, with PPO-AMBER one need not be concerned about designing the replay memory size for the proposed ER scheme, and it significantly enhances the overall performance. We also compared the performance of PPO-AMBER with other PG methods (TRPO, ACER) in Appendix 9.4, and it is observed that PPO-AMBER outperforms TRPO and ACER.

7.4 Further Discussion

It is observed that PPO-AMBER enhances the performance of tasks with low action dimensions compared to PPO by using old sample batches, but it is hard to improve tasks with high action dimensions such as Humanoid and HumanoidStandup. This is because higher action dimensions yields larger IS weights. Hence, we provide an additional IS analysis for those environments in Appendix 9.5. The analysis suggests that AMBER fits to low action dimensional tasks or sufficiently small learning rates to prevent that IS weights become too large.

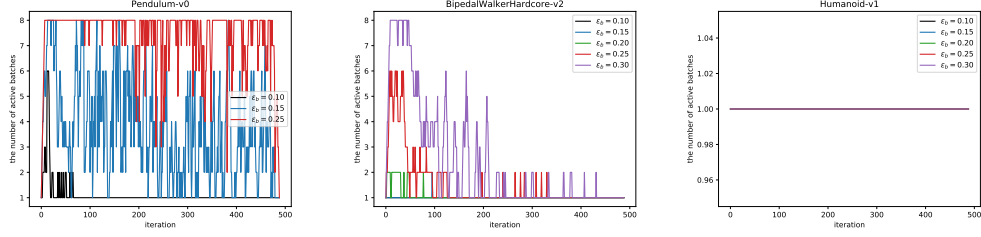


Figure 5: The number of active batches of Pendulum, BipedalWalkerHardcore, and Humanoid for PPO-AMBER with various ϵ_b

8 Conclusion

In this paper, we have proposed a MBER scheme for PPO-style IS-based PG, which significantly enhances the speed and stability of convergence on various continuous control tasks (Mujoco tasks, classic control, and Box2d on OpenAI GYM) by 1) increasing the sample efficiency without causing much bias by fixing the number of updates and reducing the IS weight, 2) reducing the sample correlation by drawing random mini-batches with the pre-computed and stored advantages and values, and 3) dropping too old samples in the replay memory adaptively. We have provided ablation studies on the proposed scheme, and numerical results show that the proposed method, PPO-AMBER, significantly outperforms original PPO.

References

- [1] Greg Brockman, Vicki Cheung, Ludwig Pettersson, Jonas Schneider, John Schulman, Jie Tang, and Wojciech Zaremba. Openai gym. *arXiv preprint arXiv:1606.01540*, 2016.
- [2] Erin Catto. Box2d: A 2d physics engine for games, 2011.
- [3] Thomas Degris, Martha White, and Richard S Sutton. Off-policy actor-critic. *arXiv preprint arXiv:1205.4839*, 2012.
- [4] Prafulla Dhariwal, Christopher Hesse, Oleg Klimov, Alex Nichol, Matthias Plappert, Alec Radford, John Schulman, Szymon Sidor, and Yuhuai Wu. Openai baselines. <https://github.com/openai/baselines>, 2017.
- [5] Scott Fujimoto, Herke van Hoof, and Dave Meger. Addressing function approximation error in actor-critic methods. *arXiv preprint arXiv:1802.09477*, 2018.
- [6] Tuomas Haarnoja, Aurick Zhou, Pieter Abbeel, and Sergey Levine. Soft actor-critic: Off-policy maximum entropy deep reinforcement learning with a stochastic actor. *arXiv preprint arXiv:1801.01290*, 2018.
- [7] Timothy P Lillicrap, Jonathan J Hunt, Alexander Pritzel, Nicolas Heess, Tom Erez, Yuval Tassa, David Silver, and Daan Wierstra. Continuous control with deep reinforcement learning. *arXiv preprint arXiv:1509.02971*, 2015.
- [8] Long-Ji Lin. Reinforcement learning for robots using neural networks. Technical report, Carnegie-Mellon Univ Pittsburgh PA School of Computer Science, 1993.
- [9] Ruishan Liu and James Zou. The effects of memory replay in reinforcement learning. *arXiv preprint arXiv:1710.06574*, 2017.
- [10] Volodymyr Mnih, Koray Kavukcuoglu, David Silver, Alex Graves, Ioannis Antonoglou, Daan Wierstra, and Martin Riedmiller. Playing atari with deep reinforcement learning. *arXiv preprint arXiv:1312.5602*, 2013.
- [11] Volodymyr Mnih, Koray Kavukcuoglu, David Silver, Andrei A Rusu, Joel Veness, Marc G Bellemare, Alex Graves, Martin Riedmiller, Andreas K Fidjeland, Georg Ostrovski, et al. Human-level control through deep reinforcement learning. *Nature*, 518(7540):529–533, 2015.
- [12] Gavin A Rummery and Mahesan Niranjan. *On-line Q-learning using connectionist systems*, volume 37. University of Cambridge, Department of Engineering, 1994.
- [13] Tom Schaul, John Quan, Ioannis Antonoglou, and David Silver. Prioritized experience replay. *arXiv preprint arXiv:1511.05952*, 2015.
- [14] John Schulman, Sergey Levine, Pieter Abbeel, Michael Jordan, and Philipp Moritz. Trust region policy optimization. In *Proceedings of the 32nd International Conference on Machine Learning (ICML-15)*, pages 1889–1897, 2015.
- [15] John Schulman, Philipp Moritz, Sergey Levine, Michael Jordan, and Pieter Abbeel. High-dimensional continuous control using generalized advantage estimation. *arXiv preprint arXiv:1506.02438*, 2015.
- [16] John Schulman, Filip Wolski, Prafulla Dhariwal, Alec Radford, and Oleg Klimov. Proximal policy optimization algorithms. *arXiv preprint arXiv:1707.06347*, 2017.
- [17] R. S. Sutton and A. G. Barto. *Reinforcement learning: An introduction*. The MIT Press, Cambridge, MA, 1998.
- [18] Richard S Sutton, David A McAllester, Satinder P Singh, and Yishay Mansour. Policy gradient methods for reinforcement learning with function approximation. In *Advances in Neural Information Processing Systems*, pages 1057–1063, 2000.
- [19] Emanuel Todorov, Tom Erez, and Yuval Tassa. Mujoco: A physics engine for model-based control. In *Intelligent Robots and Systems (IROS), 2012 IEEE/RSJ International Conference on*, pages 5026–5033. IEEE, 2012.
- [20] Ziyu Wang, Victor Bapst, Nicolas Heess, Volodymyr Mnih, Remi Munos, Koray Kavukcuoglu, and Nando de Freitas. Sample efficient actor-critic with experience replay. *arXiv preprint arXiv:1611.01224*, 2016.
- [21] Christopher JCH Watkins and Peter Dayan. Q-learning. *Machine Learning*, 8(3):279–292, 1992.

9 Appendix

9.1 Algorithm

Algorithm 1 Proximal Policy Optimization with (Adaptive) Multi-Batch Experience Replay

Require: N : batch size, M_{PPO} : mini-batch size of PPO, M : mini-batch size, L : replay length, β : step size, ϵ_b : batch drop factor, adaptive=1 or 0

- 1: Initialize $\tilde{\theta}$ and w .
- 2: Set $\theta_0 \leftarrow \tilde{\theta}$.
- 3: **for** $i = 1, 2, \dots$ (iteration) **do**
- 4: Collect the i -th trajectory $(s_{i,1}, a_{i,1}, r_{i,1}, \dots, s_{i,N}, a_{i,N}, r_{i,N})$ from π_{θ_i} .
- 5: Estimate advantage functions $\hat{A}_{i,1}, \dots, \hat{A}_{i,N}$ from the trajectory.
- 6: Estimate target values $\hat{V}_{i,1}, \dots, \hat{V}_{i,N}$ from the trajectory.
- 7: Store the i -th batch $B_i = (s_{i,n}, a_{i,n}, \hat{A}_{i,n}, \hat{V}_{i,n}, \mu_{i,n}, \sigma_i)$ at the replay memory \mathbf{R} of max size NL .
- 8: **if** adaptive **then**
- 9: **for** $l = 0, \dots, L - 1$ **do**
- 10: Compute $R'_{i,l}$ of batch B_{i-l} in the replay memory.
- 11: **if** $R'_{i,l} > 1 + \epsilon_b$ **then**
- 12: Set a batch B_{i-l} inactive
- 13: **else**
- 14: Set a batch B_{i-l} active
- 15: **end if**
- 16: **end for**
- 17: Set M as $M_{\text{PPO}} \times \#$ of active batches
- 18: **else**
- 19: Set M as $M_{\text{PPO}} \times L$, and all batches in the replay are active.
- 20: **end if**
- 21: **for** epoch $= 1, 2, \dots, S$ **do**
- 22: **for** $j = 1, 2, \dots, N/M_{\text{PPO}}$ **do**
- 23: Draw a mini-batch of M samples uniformly from the active batches.
- 24: Update the parameter as $\tilde{\theta}_{ALL} \leftarrow \tilde{\theta}_{ALL} + \beta \nabla_{\tilde{\theta}_{ALL}} \hat{L}(\tilde{\theta}_{ALL})$ from the mini-batch.
- 25: **end for**
- 26: **end for**
- 27: Set $\theta_{i+1} \leftarrow \tilde{\theta}$
- 28: **end for**

9.2 Parameter Setup

The detailed parameter setup for PPO and PPO-MBER is given in Table 2. Clipping factor ϵ of PPO and PPO-MBER varies from 0.2 to 0.7. We set ϵ of PPO-AMBER as $\epsilon = 0.4$. The batch drop factor ϵ_b is varied from 0.1 to 0.3. The mini-batch size of PPO-AMBER adaptively changes as $M = 64 \times \#$ of active batches.

Table 2: Hyperparameters of PPO, PPO-MBER, and PPO-AMBER

Hyperparameter	PPO	PPO-MBER	PPO-AMBER
Initial batch drop factor (ϵ_b)	.	.	variable
Replay length (L)	.	2, 4, 6, 8	8
mini-batch size (M)	64	$64L$	adaptive
Initial clipping factor (ϵ)	variable	variable	0.4
Horizon (N)	2048	2048	2048
Initial Adam step size (β)	$3 \cdot 10^{-4}$	$3 \cdot 10^{-4}$	$3 \cdot 10^{-4}$
Epochs (S)	10	10	10
Discount factor (γ)	0.99	0.99	0.99
TD parameter (λ)	0.95	0.95	0.95

9.3 Simulation Results

We provide the simulation results of parameter-tuned PPO, PPO-MBER, and PPO-AMBER on tasks BipedalWalker, BipedalWalkerHardcore, HalfCheetah, Hopper, Humanoid, HumanoidStandup, InvertedDoublePendulum, InvertedPendulum, Pendulum, Reacher, Swimmer, and Walker2d.

Table 3: Average return of final 100 episodes and the corresponding final ANS of parameter-tuned PPO, PPO-MBER and PPO-AMBER

	PPO	PPO-MBER ($L = 2$)	PPO-MBER ($L = 4$)	PPO-MBER ($L = 6$)	PPO-MBER ($L = 8$)	PPO-AMBER
BipedalWalker	236 ± 26	276 ± 16	275 ± 19	261 ± 13	225 ± 75	265 ± 16
BipedalWalkerHardcore	-93.5 ± 10.8	-77.9 ± 20.8	-80.7 ± 18.4	-73.2 ± 18.8	-78.1 ± 15.8	-73.5 ± 10.7
HalfCheetah	1910 ± 778	2113 ± 874	1803 ± 611	1549 ± 562	1745 ± 529	2258 ± 1039
Hopper	2185 ± 371	2063 ± 286	2135 ± 342	2095 ± 316	1850 ± 613	2213 ± 295
Humanoid	600 ± 43	578 ± 41	534 ± 34	521 ± 24	480 ± 14	613 ± 67
HumanoidStandup	82149 ± 3681	78782 ± 5620	77948 ± 3852	79004 ± 4377	77425 ± 5461	80774 ± 3518
InvertedDoublePendulum	8167 ± 630	8588 ± 271	8407 ± 305	8402 ± 209	8587 ± 208	8406 ± 363
InvertedPendulum	977 ± 20	992 ± 12	993 ± 6	987 ± 13	989 ± 11	993 ± 9
Pendulum	-683 ± 494	-463 ± 391	-286 ± 306	-161 ± 7	-160 ± 8	-155 ± 12
Reacher	-7.5 ± 2.1	-6.7 ± 2.3	-5.9 ± 1.0	-5.6 ± 0.9	-6.3 ± 0.8	-6.5 ± 1.2
Swimmer	68.4 ± 19.0	83.9 ± 21.5	92.3 ± 21.5	97.1 ± 24.5	101.6 ± 26.2	102.9 ± 26.4
Walker2d	3065 ± 532	3264 ± 577	3348 ± 498	3196 ± 429	3223 ± 445	3415 ± 416
Final ANS	0.176	0.562	0.533	0.495	0.279	0.939

Table 4: Average return of all episodes and the corresponding speed ANS of parameter-tuned PPO, PPO-MBER and PPO-AMBER

	PPO	PPO-MBER ($L = 2$)	PPO-MBER ($L = 4$)	PPO-MBER ($L = 6$)	PPO-MBER ($L = 8$)	PPO-AMBER
BipedalWalker	188 ± 29	219 ± 25	204 ± 29	198 ± 25	158 ± 64	213 ± 19
BipedalWalkerHardcore	-107.2 ± 5.3	-97.7 ± 14.6	-96.2 ± 13.6	-94.0 ± 12.6	-94.9 ± 9.3	-90.5 ± 5.7
HalfCheetah	1511 ± 583	1693 ± 630	1383 ± 365	1167 ± 367	1127 ± 234	1728 ± 709
Hopper	1736 ± 241	1604 ± 112	1761 ± 250	1750 ± 198	1390 ± 493	1719 ± 99
Humanoid	506 ± 26	495 ± 23	462 ± 19	449 ± 11	421 ± 11	504 ± 33
HumanoidStandup	77484 ± 3032	75729 ± 4806	74568 ± 3372	75486 ± 3311	73134 ± 4322	77239 ± 2857
InvertedDoublePendulum	6399 ± 442	6961 ± 296	7265 ± 131	7256 ± 153	7280 ± 115	7104 ± 99
InvertedPendulum	918 ± 12	918 ± 9	922 ± 8	926 ± 7	927 ± 3	930 ± 4
Pendulum	-751 ± 372	-567 ± 333	-421 ± 276	-288 ± 38	-279 ± 31	-272 ± 10
Reacher	-10.9 ± 1.6	-10.2 ± 2.0	-10.0 ± 0.9	-10.7 ± 0.8	-12.0 ± 0.1	-10.7 ± 1.0
Swimmer	56.2 ± 9.4	69.7 ± 16.4	75.5 ± 14.9	79.5 ± 19.6	85.3 ± 21.8	84.8 ± 20.8
Walker2d	2015 ± 400	2248 ± 403	2230 ± 424	2006 ± 299	1868 ± 313	2208 ± 320
Speed ANS	0.274	0.570	0.556	0.518	0.076	0.979

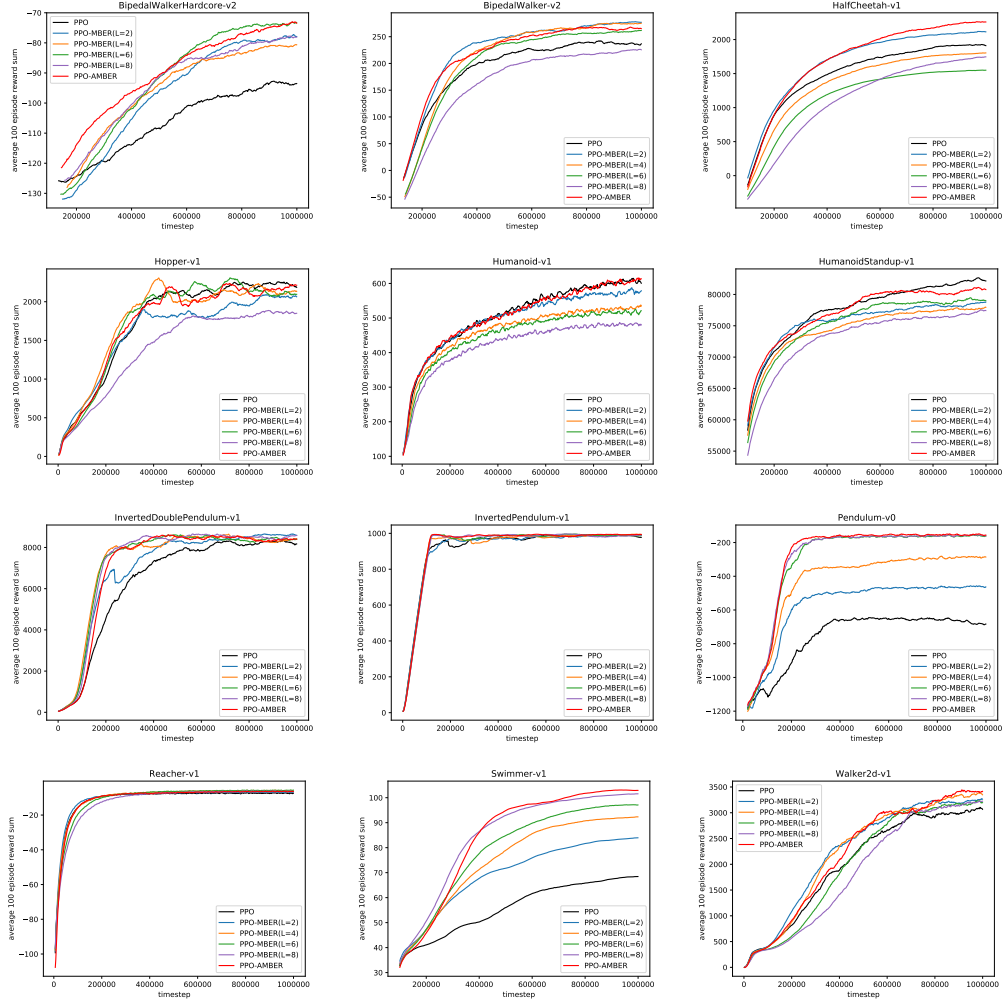


Figure 6: Performance comparison on continuous control tasks for parameter-tuned setup

Table 5: Final ANS for PPO and PPO-MBER

Clipping factor (ϵ)	PPO	PPO-MBER ($L = 2$)	PPO-MBER ($L = 4$)	PPO-MBER ($L = 6$)	PPO-MBER ($L = 8$)
0.2	-0.097	0.475	0.211	-0.070	-0.597
0.3	0.176	0.527	0.484	0.192	-0.130
0.4	-0.011	0.562	0.533	0.495	0.279
0.5	-0.678	0.236	0.116	0.148	0.110
0.6	-1.018	-0.296	0.071	-0.110	-0.068
0.7	-1.786	-0.296	-0.638	-0.843	-0.519

Table 6: Final ANS for PPO-AMBER

Batch drop factor (ϵ_b)	PPO-AMBER ($L = 8, \epsilon = 0.4$)
0.10	0.196
0.15	0.193
0.20	0.583
0.25	0.939
0.30	0.631

Table 7: Speed ANS for PPO and PPO-MBER

Clipping factor (ϵ)	PPO	PPO-MBER ($L = 2$)	PPO-MBER ($L = 4$)	PPO-MBER ($L = 6$)	PPO-MBER ($L = 8$)
0.2	-0.100	0.331	-0.190	-0.660	-1.358
0.3	0.274	0.508	0.484	0.036	-0.372
0.4	-0.002	0.570	0.556	0.518	0.076
0.5	-0.495	0.344	0.332	0.309	0.116
0.6	-0.949	-0.188	0.286	0.078	-0.032
0.7	-1.580	-0.311	-0.439	-0.536	-0.334

Table 8: Speed ANS for PPO-AMBER

Batch drop factor (ϵ_b)	PPO-AMBER ($L = 8, \epsilon = 0.4$)
0.10	0.083
0.15	0.308
0.20	0.688
0.25	0.979
0.30	0.671

9.4 Performance Comparison with Other IS-based PG Methods

Since the paper considers the performance improvement for IS-based PG methods based on ER, we compared proposed PPO-AMBER with other IS-based PG methods: TRPO and ACER. We used the single-path TRPO of OpenAI baselines and our own ACER which is a modified version from the discrete ACER in OpenAI baselines. The policy networks of both algorithms were a Gaussian policy which was the same as that of PPO. For TRPO, the batch size was 1024 and the KL step size was 0.01. Note that the batch size and the performance of TRPO fit to 1M time-step simulation as seen in the result comparison in [16]. For ACER, the stochastic dueling network with 2 hidden layers of size 64 and $n = 5$ [20] was used for the value network, and we used the fixed learning rate $7 \cdot 10^{-4}$ and the KL step size 0.1. Other parameters of ACER were the same as [20]. The result is given in Fig. 7. It is seen that PPO-AMBER outperforms TRPO and ACER.

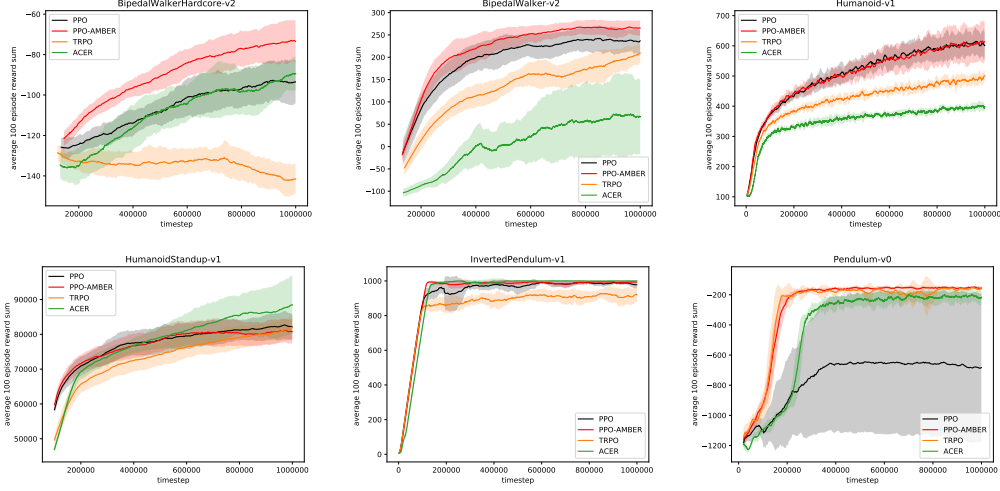


Figure 7: Performance comparison with other IS-based PG methods

9.5 IS Analysis on High Action-Dimensional Tasks

The different dimensions of the action spaces of different tasks much affect different IS weights for different tasks. The IS weight can be factorized as $R_t(\tilde{\theta}) = \frac{\pi_{\tilde{\theta}}(a_t|s_t)}{\pi_{\theta}(a_t|s_t)} = \prod_{k=1}^K \frac{\pi_{\tilde{\theta}}(a_{t,k}|s_t)}{\pi_{\theta}(a_{t,k}|s_t)}$, where K is the action dimension, $a_{t,k}$ is the k -th element of a_t , and $\pi_{\theta}(a_{t,k}|s_t) = \frac{1}{\sqrt{(2\pi)\sigma_k}} \exp(-(\mu(s_t; \phi)_k - a_{t,k})^2/2\sigma_k^2)$. Thus, the IS weight increases as K increases, if the change of μ_k and σ_k is similar for each action dimension. Fig. 3 shows this behavior (the action dimension - Pendulum : 1, BipedalWalkerHardcore : 4, Humanoid : 17). Hence, the IS weight for Humanoid for old samples is too large and using the current sample only is best for Humanoid (and HumanoidStandup). With $\epsilon_b = 0.25$ across all tasks, samples with the IS weight larger than 1.25 are not used. Note that small learning rates reduce the change of μ_k and σ_k , and consequently reduce the IS weight. Hence, in order to apply AMBER to the harder tasks with high action dimensions, we consider reducing the learning rate from $(3 \cdot 10^{-4})$ to $(4 \cdot 10^{-5})$ and re-applying AMBER. The result is shown in Fig. 9.5. As expected, AMBER with the small learning rate uses a larger number of batches than the original AMBER due to the reduced IS weights, and AMBER improves the performance of PPO with the small learning rate. However, the performance behavior of PPO-AMBER is different for tasks. For Humanoid, reducing the learning rate harms the performance more than the improvement by AMBER. So, the overall performance with the reduced learning rate is worse. On the other hand, for HumanoidStandup, reducing the learning rate enhances the performance, and AMBER further improves the performance. These results suggest that AMBER is efficient for small action-dimension tasks or sufficiently small learning rates so that IS weights are not too large.

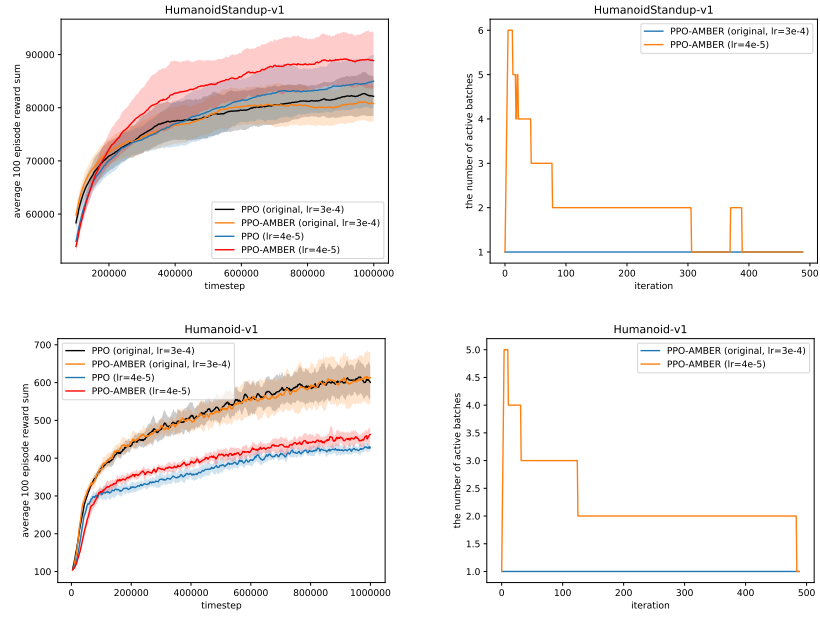


Figure 8: The evaluation of AMBER and the corresponding number of active batches